Rapid prototyping of microfluidic devices for integrating with FT-IR spectroscopic imaging

K. L. Andrew Chan,[a] Xize Niu,[b] Andrew J. de Mello[b] and Sergei G. Kazarian*[a]

Received 15th March 2010, Accepted 28th April 2010
DOI: 10.1039/c004246c

A versatile approach for the rapid prototyping of microfluidic devices suitable for use with FT-IR spectroscopic imaging is introduced. Device manufacture is based on the direct printing of paraffin onto the surface of an infrared transparent substrate, followed by encapsulation. Key features of this approach are low running costs, rapid production times, simplicity of design modifications and suitability for integration with FT-IR spectroscopic measurements. In the current experiments, the minimum width of channel walls was found to be ~120 μm and ~200 when a 25 μm and 12 μm spacer is used, respectively. Water and poly(ethylene glycol) are used as model fluids in a laminar flow regime, and are imaged in both transmission and attenuated total reflection (ATR) modes. It is established that adoption of transmission mode measurements yields superior sensitivity whilst the ATR mode is more suitable for quantitative analysis using strong spectral absorption bands. Results indicate that devices manufactured using this approach are suitable for use with *in situ* FT-IR spectroscopic imaging.

Introduction

Microfabrication of microfluidic devices typically involves the use of materials such as poly(dimethylsiloxane) (PDMS), poly-(methylmethacrylate) (PMMA) or glass due to the ease of fabrication, low manufacturing costs and the optically transparency of the resulting substrates in the UV/visible part of the electromagnetic spectrum. Detection methods most normally involve optical techniques such as absorption spectroscopy and fluorescence spectroscopy. However, UV and visible absorption methods lack chemical specificity while fluorescence-based methods rely on the existence of a suitable tag that can be attached to the molecule of interest. Additionally, there are significant challenges associated with the detection of small molecules by fluorescence since the properties of a small molecule can be significantly altered by the presence of an extrinsic tag. Nevertheless, the high spatial resolution, single molecule level limits of detection[1] and fast image acquisition make it the most popular detection method for microfluidic analysis.

Fourier Transform Infrared (FT-IR) spectroscopy, despite its relatively low spatial resolution, provides rich and label-free chemical information about molecular systems. Indeed the development of FT-IR spectroscopic imaging will undoubtedly provide a spatial dimension of information that is crucial in the microfluidic analysis. Although the method does not require any labelling, most polymeric and glassy substrates are not transparent in the mid-IR region which contains most of the information required for molecular analysis. Our recent studies demonstrated that the integration of PDMS devices with attenuated total reflection-FT-IR (ATR-FT-IR) imaging could be used to analyse fluid flow in microfluidic channels, where the measuring surface of the internal reflection element (IRE) was used as the base of the microfluidic device.[2] In that study, PDMS devices were produced by standard lithographic fabrication methods.[3] Using this approach, fluids that came into contact or were in close proximity (within 2 μm micrometers) to the IRE could be measured. Other studies by Holman *et al.*[4] employed an infrared reflective substrate as the base of the microfluidic device and an open channel approach to capture FT-IR maps of biofilms with a synchrotron source in transflection mode. However, it was challenging to maintain laminar flow and achieve appropriate pathlengths through aqueous samples which requires the balancing between the hydrostatic pressure at the inlet and outlet. Closed infrared transparent capillaries have also been fabricated for on-chip infrared detection, where calcium fluoride windows were etched.[5]

Herein we present a fast, simple but effective approach for the rapid prototyping of microfluidic device with closed channels that are suitable for FT-IR imaging. The devices manufactured using this method may also be applicable to other detection methods. We have previously shown that a microdroplet system can be employed to print wax pattern that confine liquids on surfaces.[6,7] The idea here is to create a microfluidic device by printing the designed pattern using molten wax (which solidifies at room temperature) directly onto the surface of IR transparent crystals; for example the surface of CaF_2 windows of a standard infrared transparent liquid cell or the measuring surface of an inverted prism of an ATR imaging accessory. The paraffin can be cleaned without damaging the substrate, thus allowing the infrared transparent window or crystal to be used multiple times. Additionally changes in the microfluidic design can be easily implemented and new designs made within minutes. Direct printing of patterns onto substrates using laser etching (for microfluidic device fabrication) has been demonstrated previously.[8] However, the obvious disadvantage of such an approach is that the substrate is permanently marked and is unsuitable for reuse. It should be noted that devices created *via* wax printing

[a]*Department of Chemical Engineering, Imperial College London, SW7 2AZ, United Kingdom. E-mail: s.kazarian@imperial.ac.uk; Tel: +44 (0)20 7594 5574*
[b]*Department of Chemistry, Imperial College London, SW7 2AZ*

will be limited to the study fluids that do not dissolve the wax. However, other materials or coating techniques may be further developed to refine the approach presented here if the study involves the use of wax-dissolving solvents. Finally, it should also be noted that microfluidic devices have previously been manufactured by direct printing paraffin onto paper.[9] However, the fluid transport in these devices is through paper while in this study, the fluid transport occurs through the fabricated channels.

Experimental

Microdroplet system

The microdroplet-on-demand device (AutoDrop®, MicroDrop) consists of a *xyz* control unit, a heated dispensing nozzle head with heated reservoir, a *xyz* position robotic arm and a built-in computer. Paraffin was heated to 90 °C in the reservoir to initiate melting, and the nozzle head was maintained at 80 °C during the deposition process. Paraffin walls were created by printing drops adjacent to each other with a separation of 50 μm.

Microfluidic devices

The design chosen to demonstrate the feasibility of the fabrication method consists of two channels (one 300 μm wide and the other at 400 μm wide) which meet at a 90° junction. The mixing channel (400 μm wide) includes a serpentine section with two 90° turns and three 180° turns, as shown in Fig. 1. Water was introduced through the wider channel whilst PEG was introduced through the narrower channels.

Transmission FT-IR imaging

FT-IR imaging was performed on a continuous scan FT-IR spectrometer (Varian 670-IR, Varian Inc., USA) with a large sample compartment (Varian Inc., USA) attachment. A horizontal macro transmission accessory was employed to allow the device to be measured as a transmission cell on a horizontal position. Further details about this accessory can be found elsewhere.[10] No magnification is expected for this optical system. A 128 × 128 focal plane array detector (40 μm per pixel) was used in all experiments. The region of interest was found to fit within the image captured by the 96 × 96 pixels. The imaging area under this setup is therefore 3.84 mm × 3.84 mm with a nominal spatial resolution of 40 μm. Spectra were measured at 8 cm^{-1} resolution with 32 co-additions resulting in a total scanning time of approximately 40s per image. A CaF_2 liquid cell with 25 and 12 μm poly(ethylene terephthalate) spacers (Omni Cell, Specac Ltd., UK) was used as the substrate. The exits of the window were connected to poly(ethylene) tubing for injection of fluid into the device. Precision syringe pumps (PHD 2000, Harvard Apparatus) were used to deliver the fluids into the channel network. Deionised water and poly(ethylene) glycol 200 (Sigma Aldrich) were chosen as model fluids and used as received.

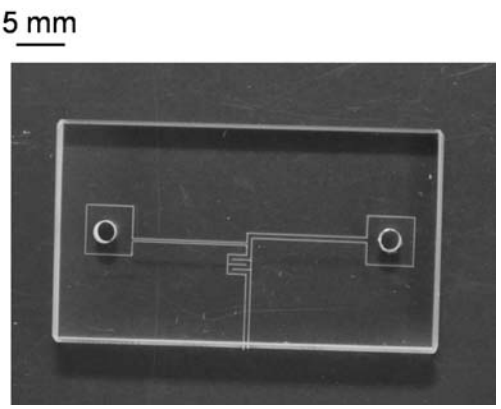

Fig. 1 Photograph of a printed paraffin pattern on a CaF_2 window. The white lines are made of paraffin drops.

ATR-FT-IR imaging

The spectral measurement is exactly the same as the transmission experimental setup. However, instead of the horizontal macro transmission accessory, a 45° single reflection inverted ATR prism made of ZnSe (PIKE Technologies, USA) with a 20 mm diameter sampling surface was used. The ATR prism is placed on an optical box where two adjustable flat mirrors are used to direct IR radiation to the IRE and the internally reflected light to the detector.

Results and discussion

Transmission FT-IR imaging

Fig. 1 shows a representative paraffin printed microfluidic device before encapsulation. The channel walls are built from droplets of paraffin and the CaF_2 window is unaffected by the deposition process. There were only 2 holes on the original CaF_2 window

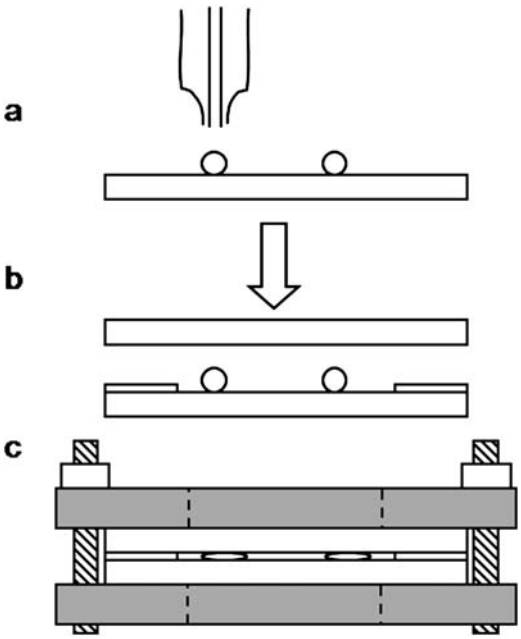

Fig. 2 Schematic showing the fabrication of a microfluidic device. (a) A paraffin pattern is printed directly onto the surface of the infrared transparent window of the liquid cell. (b) The printed pattern is sandwiched between two windows together with a suitable spacer. (c) The windows are held together with the frame of the liquid cell.

(standard for infrared transparent liquid cells) therefore a collection stream was not included in the design. Nevertheless, this does not prevent demonstration of the idea, and indeed it is possible to drill additional holes in the window to maximise flexibility.

The processes involved in creating microfluidic devices are summarised in Fig. 2. First, the microfluidic design was programmed on the microdroplet system as a set of co-ordinates. A macro program was written such that the microdroplet system deposits droplets of paraffin at precise locations according to these coordinates. A spacer of suitable thickness (either 25 μm or 12 μm in this study) was placed around the paraffin pattern. Finally the paraffin pattern was sandwiched between the two CaF_2 windows and pressure applied until the spacing between the windows became the same as the thickness of the spacer. The paraffin compresses and forms a seal between the two windows creating a closed microfluidic channel (Fig. 2c).

The size of a dispensed paraffin droplet is typically 65 μm in diameter and increases to approximately 200 μm when sandwiched between windows with a 12 μm spacer. This dimension determines the width of the channel wall achievable using this approach. Thicker walls can be created by aligning two rows of paraffin droplets in parallel or by using a thinner spacer. When a 25 μm spacer is used, the wall width decreases to approximately 120 μm. However, our experiments indicate that even a single layer wall of 120 μm width (25 μm spacer) is strong enough to withstand the pressure from the fluid flow conditions employed in this experiment. The smallest channel width is limited by the accuracy of the *xyz* positioning robotic arm which for the current system is ~40 μm and is similar to the spatial resolution provided by this optical arrangement. The imaging spatial resolution can be increased to between 10–20 μm by adaptation of the infrared microscope, but occurs at the expense of a reduced field of view (depending on the power of magnification of the microscope). An image of a device with 12 μm spacer based on the $\delta(CH)_2$ absorbance of paraffin captured using the imaging spectrometer is shown in Fig. 3a. For devices with a thicker spacer, and thus a greater channel height, the channel is approximately 80 μm wider due to the paraffin wall being less spread when pressed.

Fig. 3b illustrates a device containing a water flow. The image is generated based on the water absorbance at 1640 cm^{-1}

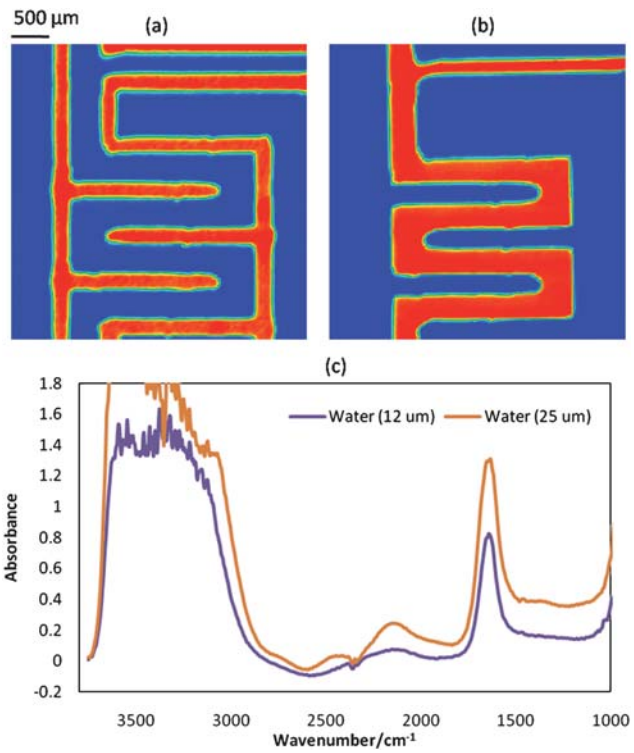

Fig. 3 (a) Image of the paraffin device (12 μm thick spacer) based on the absorbance of paraffin band at 1462 cm^{-1}. (b) Image of the same device filled with water. Image generated based on the absorbance of water at 1640 cm^{-1}. (c) Extracted spectra from inside the channel with water flowing continuously inside.

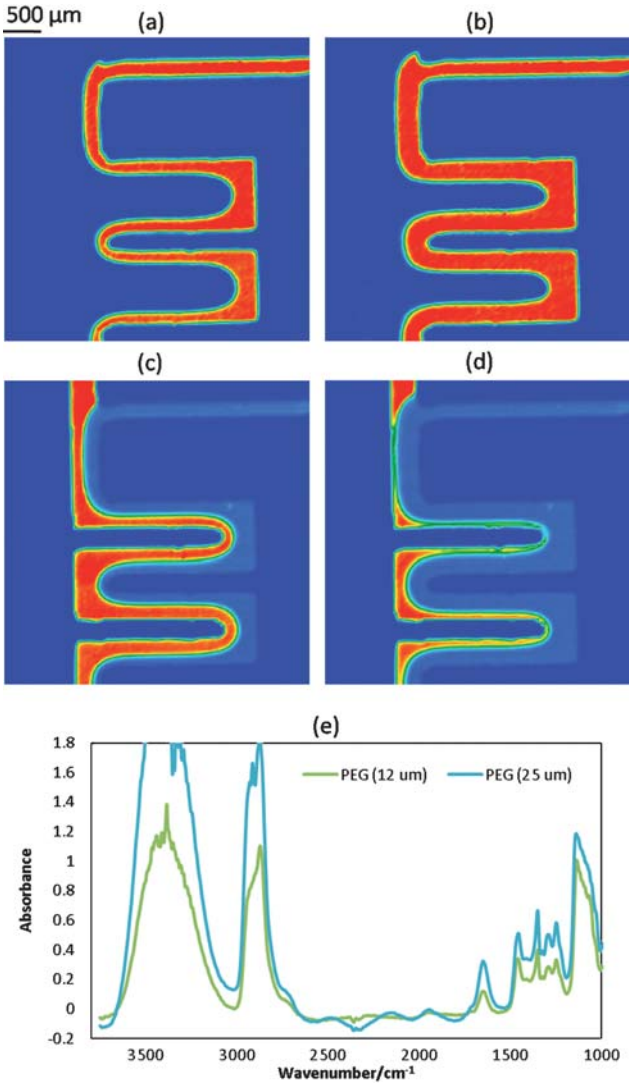

Fig. 4 (a) and (b) illustrate FT-IR images of the flow pattern of PEG 200 (12 μm thick spacer) based on the absorbance of the band at 1350 cm^{-1} at a flow rate of PEG 200 of 1 μl/min against a flow rate of water of (a) 10 μl/min and (b) 2 μl/min. (c) and (d) present FT-IR images of the flow pattern of water (12 μm thick spacer) based on the absorbance of the band at 1640 cm^{-1} with a flow rate of water of (c) 10 μl/min and (d) 2 μl/min against a flow rate of PEG 200 of 1 μl/min. (e) Extracted spectra from inside the channel of devices with 12 μm and 25 μm thick spacers in the PEG 200 rich region.

due to the bending vibrational mode. The image shows that the water stream flows only inside the channel and no leakage is observed. Similar experiments performed using a device with a 25 μm spacer (image not shown) also demonstrate no leakage. Spectra were extracted from a region inside the channel with both the 12 μm and 25 μm thick spacers and presented in Fig. 3c. For quantitative analysis, spectral bands should typically have an absorbance of less than 0.8 to ensure a linear detection response. The recorded absorbance of water bands for the 25 μm thick spacer device are very strong between 3700 cm^{-1}–3000 cm^{-1} and 1700 cm^{-1}–1600 cm^{-1}, making it difficult to perform quantitative analysis in these spectral regions. However, quantitative analysis may be possible for molecules that absorb in the regions where water does not absorb infrared radiation strongly (*e.g.* between 2900–1800 cm^{-1} and 1500–1000 cm^{-1}). The spectrum extracted for the device containing the 12 μm spacer shows that the band corresponding to the bending mode of water is relatively weak while the OH stretching bands remain off-scale. Importantly, the rest of the spectral region is open for analysis in a quantitative manner.

To demonstrate that laminar flow can be established and controlled with this type of device, mixing of water with PEG 200 at a T-junction under different water flow rates was performed. Fig. 4a and 4c show the flow pattern of PEG 200 and water at respective volumetric flow rates of 1 μl/min and 10 μl/min. Water enters the device from the top and PEG from the right hand side. Despite the fact that the volumetric flow rate of water is 10 times higher than the flow rate of PEG 200, the share of the channel dimension between the two fluids remains similar. This is due to the higher viscosity of PEG 200 compared to water and is consistent with previous observations.[2] Fig. 4b and 4d show the flow pattern of PEG 200 and water when the flow rate of water is reduced to 2 μl/min while the flow rate of PEG remains the same. The channel is now mostly occupied by PEG 200 while water is confined to the left side of the channel as expected. In both cases, the results show that the laminar flow pattern is maintained. Spectra extracted from the PEG 200 rich region of the channel are shown in Fig. 4e. The spectra indicate that although the absorbance of the bands at 3300 cm^{-1}, 2850 cm^{-1} and 1120 cm^{-1} are very strong and provide mostly qualitative information, quantitative analysis remain possible in most parts of the spectral

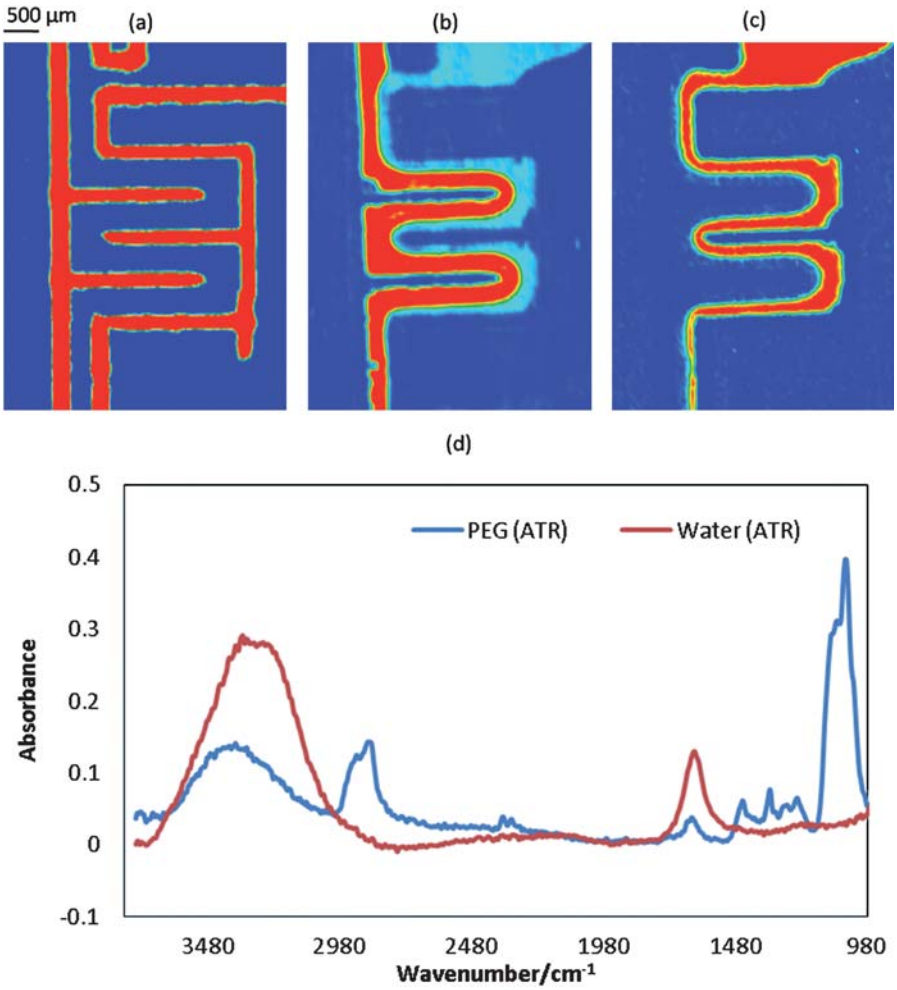

Fig. 5 (a) ATR-FT-IR image of a paraffin device mounted on the ATR accessory based on the absorbance of paraffin at 1462 cm^{-1}. (b) and (c) are the ATR-FT-IR images of the flow pattern of water and PEG 200 flowing in the channel at a flow rate of 5 μl/min of water and 1 μl/min of PEG 200. (d) Extracted spectra from inside the channel in the PEG 200 and water rich region.

region between 2800 cm^{-1} and 1150 cm^{-1}. This experiment clearly demonstrates that direct deposition of paraffin to create microfluidic devices can be an effective, fast and a cost-effective option for microfluidic analysis using FT-IR imaging.

ATR-FT-IR imaging

In addition to a transmission geometry, the direct printing method is also suitable for use with ATR-FT-IR imaging. ATR-FT-IR imaging offers the benefits of a sample thickness independent pathlength, making it an ideal sampling method for the analysis of samples in an aqueous environment. As Fig. 3c demonstrates, water absorbs strongly in broad mid-IR regions, and thus the ability to generate a controlled and small (typically a few μm) pathlength is crucial when quantitative analysis is required. While our previous demonstration of imaging microfluidic channels with ATR-FT-IR involved the use of a PDMS device, this new approach offers more convenience and speed. As described previously, the sealing between the PDMS and the IRE relies on the adherence of the two surfaces. The seal was reinforced by pressing the PDMS against the IRE. However, the pressure applied is limited by the need to avoid significant deformation of the PDMS and hence the cross-sectional shape of the channel. With the paraffin printing approach described herein, channels are created by pressing a transparent PMMA slab onto the printed pattern on the measuring surface of the IRE with an appropriate spacer. Since an elastomer is not used, higher pressures can be applied and a better seal made. A similar experiment to the transmission FT-IR imaging of laminar flow was performed with the ATR geometry. Fig. 5 shows results measured in ATR mode with flow rates of PEG 200 and water of 1 μl/min and 5 μl/min respectively. The paraffin distribution image which depicts the microfluidic device (Fig. 5a) shows that the design is slightly different to the one created for imaging in transmission. The design was modified slightly due to the difference in size of the ATR surface compared to the transmission cell. Furthermore, the image appears to be elongated along the *y*-axis (the vertical axis) when compared to Fig. 3a despite the same detector and number of pixels being used. This has been explained in previous studies and occurs as a result of the light projected through an ATR prism with a 45° incident angle.[11,12] Fig. 5b and 5c illustrate the flow pattern of water and PEG 200. It should be noted that the diagonal line on the top right corner of the image is a result of air being trapped in the reservoir of the PEG inlet. The flow pattern generally replicates what is observed in the transmission microfluidic cell, thus demonstrating that the paraffin printing approach is suitable for ATR measurements. Spectra extracted from the PEG 200 rich region and water region are shown in Fig. 5c. All spectral bands have an absorbance less than 0.4 which is ideal for quantitative analysis. However, due to the small pathlength provided by this method the signal to noise ratio (SNR) is not as good as that observed in transmission mode. The SNR is especially important for analytes at low concentration and determines the detection limit. For example, for the PEG 200 band at 1350 cm^{-1}, the peak to peak signal was ~0.075 while the noise level (measured at 1900 cm^{-1}) was ~0.004 which gives a SNR of ~19 when measured in ATR mode. The SNR for the same band in transmission mode with a 12 μm spacer and the same scanning time is ~200. Further improvement on the SNR may be achieved by increasing the scanning time or averaging spectra from the imaging pixels.

Conclusions

A new type of microfluidic device that is suitable for infrared spectroscopic imaging analysis has been developed and demonstrated by analysis of the laminar flow of water and PEG 200 in microchannels. The device is based on the direct printing of paraffin droplets to create the walls for the microfluidic channels on the window surface of a standard infrared transmission liquid cell or on the surface of the IRE. The advantages of this approach include: the fact that the device can be printed in minutes, the design of the device can be altered easily and new devices can be printed immediately. The relatively expensive infrared transparent windows and accessory can be reused for multiple experiments which results in a very low consumable cost. The minimum wall thickness is ~120 μm while the minimum width for the channel is ~40 μm, which is similar to the spatial resolution of the macro FT-IR imaging system in transmission mode. FT-IR imaging in transmission using 25 μm and 12 μm thick spacers was found to yield spectra with higher signal to noise ratios (and thus better sensitivity) than for ATR-FT-IR imaging, while the ATR measurement is better suited for measuring samples with strong spectral bands such as water. [13]

Acknowledgements

SGK acknowledges the research funding from the European Research Council under the *European Community's* Seventh Framework Programme (*FP7/2007–2013*)/ERC *advanced grant agreement* n° [*227950*]. XN acknowledges support from the RCUK Microdroplets Basic Technology Project (EP/D048664/1).

References

1 E. K. Hill and A. J. de Mello, *Analyst*, 2000, **125**, 1033–1036.
2 K. L. A. Chan, S. Gulati, J. B. Edel, A. J. de Mello and S. G. Kazarian, *Lab Chip*, 2009, **9**, 2909–2913.
3 D. C. Duffy, J. C. McDonald, O. J. A. Schueller and G. M. Whitesides, *Anal. Chem.*, 1998, **70**, 4974–4984.
4 H. Y. N. Holman, R. Miles, Z. Hao, E. Wozei, L. M. Anderson and H. Yang, *Anal. Chem.*, 2009, **81**, 8564–8570.
5 T. Pan, R. T. Kelly, M. C. Asplund and A. T. Woolley, in *26th International Symposium on Capillary Chrmatography and Electrophoresis*, Elsevier Science Bv, Las Vegas, Nevada, 2003, pp. 231–235.
6 J. M. Andanson, K. L. A. Chan and S. G. Kazarian, *Appl. Spectrosc.*, 2009, **63**, 512–517.
7 K. L. A. Chan, L. Govada, R. M. Bill, N. E. Chayen and S. G. Kazarian, *Anal. Chem.*, 2009, **81**, 3769–3775.
8 J. Y. Cheng, C. W. Wei, K. H. Hsu and T. H. Young, *Sens. Actuators, B*, 2004, **99**, 186–196.
9 Y. Lu, W. W. Shi, L. Jiang, J. H. Qin and B. C. Lin, *Electrophoresis*, 2009, **30**, 1497–1500.
10 K. L. A. Chan and S. G. Kazarian, *Vib. Spectrosc.*, 2006, **42**, 130–134.
11 A. Nakamura, T. Koga, M. Fujimaki, Y. Ohki, T. Sota, K. Lipinska-Kalita, T. Nagae, S. Ishimaru and K. Aizawa, *Jpn. J. Appl. Phys.*, 2000, **39**, 490–492.
12 K. L. A. Chan and S. G. Kazarian, *Appl. Spectrosc.*, 2003, **57**, 381–389.
13 S. G. Kazarian and K. L. A. Chan, *Appl. Spectrosc.*, 2010, **64**, 135A–152A.

